Journal of Power Sources 233 (2013) 62–68

Contents lists available at SciVerse ScienceDirect

Journal of Power Sources

journal homepage: www.elsevier.com/locate/jpowsour

NiCu–$Zr_{0.1}Ce_{0.9}O_{2-\delta}$ anode materials for intermediate temperature solid oxide fuel cells using hydrocarbon fuels

Shidong Song, Minfang Han*, Jianqiang Zhang, Hui Fan

Union Research Center of Fuel Cell, School of Chemical and Environment Engineering, China University of Mining and Technology, Beijing 100083, PR China

HIGHLIGHTS

- By doping Zr into ceria, thermal stabilities and activities of anodes are improved.
- The best performing anode is Ni–$Zr_{0.1}Ce_{0.9}O_{2-\delta}$ cermet.
- The best thermally stable anode is Cu–$Zr_{0.1}Ce_{0.9}O_{2-\delta}$ cermet.
- $Ni_{0.5}Cu_{0.5}$–$Zr_{0.1}Ce_{0.9}O_{2-\delta}$ anode achieves both high stability and high activity.
- Ni–Cu alloy–Zr doped CeO_2 can be promising candidate anode materials.

ARTICLE INFO

Article history:
Received 10 October 2012
Received in revised form
2 January 2013
Accepted 3 January 2013
Available online 12 January 2013

Keywords:
Solid oxide fuel cell
Anode
Ceria–zirconia
Intermediate temperature
Direct utilization of hydrocarbons

ABSTRACT

NiCu–$Zr_{0.1}Ce_{0.9}O_{2-\delta}$ based cermets are evaluated as anode materials for intermediate temperature solid oxide fuel cells (IT-SOFCs) using hydrocarbon fuels. Polarization curves and stability tests are conducted for direct methane SOFCs with various anode materials at 700 °C. The performances and thermal stabilities of the cells with $Zr_{0.1}Ce_{0.9}O_{2-\delta}$ based anodes are significantly higher than those using pure CeO_2-based anodes, indicating by doping 10 mol% Zr into CeO_2, the thermal stability and anode performance can be improved. Among the anode materials investigated, the best performing anode is Ni–$Zr_{0.1}Ce_{0.9}O_{2-\delta}$. The cell using the $Ni_{0.5}Cu_{0.5}$–$Zr_{0.1}Ce_{0.9}O_{2-\delta}$ anode exhibits a similar performance to that with the Ni–$Zr_{0.1}Ce_{0.9}O_{2-\delta}$ anode, but experiences a much lower degradation after a short-term operation in weakly humidified CH_4. The cell using the Cu–$Zr_{0.1}Ce_{0.9}O_{2-\delta}$ anode shows the best stability, only 0.61% degradation after a 48 h operation, but a low performance as well. The results suggest that NiCu–$Zr_{0.1}Ce_{0.9}O_{2-\delta}$ based cermets could be promising candidate anodes for direct hydrocarbon IT-SOFCs.

1. Introduction

Solid oxide fuel cells (SOFCs) are electrochemical devices that directly convert the chemical energy of a fuel into electrical energy with high efficiency and low emission of pollutants. Though hydrogen represents an attractive clean fuel it is not readily available and its storage and transportation still present technological hurdles. Thus, direct utilization of hydrocarbons in SOFCs based on oxide ion conducting electrolytes would contribute to the more effective utilization of remaining fossil fuel reserves [1–3]. Anode materials are regarded as one of the most important components for direct hydrocarbon SOFCs. Ideally, the direct utilization of hydrocarbons without reforming, either external or internal, at anodes can not only enhance the fuel cell efficiency but also simplify the system. However, the conventional anode material for SOFCs, Ni–YSZ cermet, cannot be used for this application directly since Ni is a good catalyst for hydrocarbon cracking reaction [1]. Different alternatives such as Ni-, Cu–CeO_2-based cermets [4,5] and various perovskites [6–8] have been developed to overcome such deactivating effect for direct hydrocarbon SOFCs. Though perovskite anodes exhibit good resistances to carbon deposition and tolerances to sulfur contamination, their electrical conductivity and electro-catalytic activity are still lower than those of cermet anodes under the reducing environments. Ni–, Cu–CeO_2-based cermets have been widely studied and showed significant activities for direct utilization of hydrocarbon fuels in SOFCs [2–5]. Furthermore, these CeO_2-containing anodes can be easily compatible with electrolytes able to operate at intermediate temperatures like gadolinium-doped ceria (GDC) [1]. Murray et al. [2] have successfully operated a cell on dry methane by employing

* Corresponding author.
E-mail address: hanminfang@sina.com (M. Han).

0378-7753/$ – see front matter © 2013 Elsevier B.V. All rights reserved.
http://dx.doi.org/10.1016/j.jpowsour.2013.01.022

a nickel-containing CeO_2-based anode. Recently, the use of Cu–CeO_2 anodes has received much attention for direct utilization of a large diversity of hydrocarbons in SOFCs [4,5]. Cu is generally chosen as the electronic conductor due to its catalytic inertness for carbon formation. CeO_2 acts as an oxidation catalyst and a mixed ionic-electronic conductor (MIEC) under reducing conditions.

The catalytic activities of Ni-, Cu–CeO_2-based anodes strongly depend on the interaction between metal and oxide, that is, the strong metal–support interaction (SMSI). However, CeO_2 has the disadvantage of being less refractory, causing the loss of SMSI and catalytic activity at a relatively high temperature. He et al. [9] found that the area-specific resistance (ASR) of an SOFC using CeO_2 anode sintered at 723 K was about three times lower than that sintered at 1523 K. This was attributed to a loss of CeO_2 surface area due to particle sintering. Furthermore, under a reducing condition, the relatively big effective ionic radius of Ce^{3+} (0.114 nm) compared to that of Ce^{4+} (0.097 nm) can cause an expansion of the CeO_2 lattice and a concomitant structure instability [10]. One way to counteract this would be to add metal ions into CeO_2. Most of the related studies were on the substitution of a lower-valent metal ion, such as Tb^{3+} [11], Fe^{2+} [12,13] or Sm^{3+} [14] for Ce^{4+}. Doping CeO_2 with Tb^{3+} results in a lowering of the energy barrier for oxygen migration and a stabilization of specific surface area during high temperature calcinations [11]. But Ce seems to be less reducible to Ce^{3+} in the presence of Tb^{3+} and its electrical conductivity is rather low under reducing conditions, possibly due to the excess electrons being located on Tb in preference to Ce. Pe'rez-Alonso et al. [12] studied the chemical structures of co-precipitated Ce–Fe mixed oxides. They thought that these Ce–Fe mixed oxides were not suitable to become anode materials for SOFCs because doping CeO_2 with high Fe content induces the extremely low oxygen vacancy concentration [13]. Tavares et al. [14] studied Cu–$Ce_{0.8}Sm_{0.2}O_{1.9}$ (Cu-SDC) anode material for IT-SOFC and achieved an excellent cell performance in methane. However, the short-term stability tests showed an initial impairment of the anode performance and carbon formation.

Adding small Zr^{4+} (0.084 nm) into CeO_2 has proven very useful in stabilizing CeO_2 for oxidation or partial oxidation reaction of hydrocarbons [10]. The dissolution of ZrO_2 into the cubic fluorite lattice of CeO_2 strongly affects its catalytic behavior by lowering the activation energy for oxygen mobility within the lattice. This results in an increase in the oxygen storage capacity (OSC) and the concentration of Ce^{3+} which acts as the active site for oxidation of hydrocarbon [10,15]. Zr doped CeO_2 (ZDC) have exhibited a stable activity for direct oxidation of methane without carbon deposition at temperatures below 800 °C [16]. Larrondo et al. [16] examined the catalytic activity of ZDC for direct oxidation of methane by TPR method, aiming at their potential applications as anode materials for direct hydrocarbon SOFCs. They concluded that Zr can stabilize the reducibility of both surface and bulk CeO_2 sites. Ahn et al. [17] investigated the SOFC performance using Cu–$Zr_{0.4}Ce_{0.6}O_2$–YSZ anode material compared with that using Cu–CeO_2–YSZ anode. The latter showed a lower performance after both anode materials were calcined at 1273 K. Recently, Cimenti et al. [18] have investigated the direct utilization of methanol in SOFCs with impregnated Ni/YSZ and Ni–$Zr_{0.35}Ce_{0.65}O_2$/YSZ anodes at 1073 K. The performances and stabilities of anodes were remarkably improved by the presence of ZDC. The carbon deposition could be effectively mitigated by ZDC, whether the cells were operated at open circuit or under load (at 0.6 V). Though the CeO_2-based anodes have been studied extensively for direct hydrocarbon SOFCs, to the best of our knowledge, the investigations on use of ZDC anodes are rare. Baker et al. [19] have reported that by doping Zr into CeO_2 both the anode performance and thermal stability could be largely improved. The anode polarization could be reduced by more than half for ZDC electrodes with low Zr contents ($Zr_{0.1}Ce_{0.9}O_2$ and $Zr_{0.25}Ce_{0.75}O_2$), possibly due to the Zr^{4+} helping to enhance surface and bulk oxygen species mobility and the concentration of Ce^{3+} [20]. Therefore, a strategy of developing CeO_2-based anodes with good thermal stability and catalytic activity through doping with Zr would worth further pursuing.

Since the electronic conductivity of CeO_2 at intermediate temperatures is not adequate for use as anodes for SOFCs, and its anode performance can be largely enhanced by adding a catalytic component for C–H bond breaking in CH_4, the use of an active metal phase is necessary for CeO_2-based anode. The coupling of metal such as Ni, Cu and alloys with CeO_2 can provide enough electronic conductivity for the anodes and enhance the oxidation rate of hydrocarbons [21–23]. In contrast to Ni, Cu does not catalyze the cracking process and is effective as current collector under reducing conditions. However, Cu has several limitations related to its relatively low melting temperature, which makes the fabrication of Cu–CeO_2-based anodes difficult and limits the SOFC operation temperature to below intermediate temperature. Furthermore, Cu is also rather poor for hydrocarbon activation [24]. One approach for enhancing the catalytic properties of Cu and stabilizing the tendency of Ni for carbon formation is to use Ni–Cu alloys. Ni–Cu alloy–CeO_2-based anodes offer potential advantages with respect to typical Ni–YSZ anode for direct hydrocarbon SOFCs [21–23,25,26]. In the present work, we investigated the performances and stabilities of NiCu–$Zr_{0.1}Ce_{0.9}O_2$ based anodes for direct methane IT-SOFCs using GDC electrolytes at 700 °C, with NiCu–CeO_2-based anode as the reference material. Using GDC as the electrolyte gives the advantages of higher electrolyte conductivity, better adhesion, and thermal and chemical matching to the $Zr_{0.1}Ce_{0.9}O_2$ materials. The effects of the promotion by Ni–Cu alloy on electrochemical activity and stability for the anodes are also examined. This work extends the previous impedance studies on ZDC anode materials for direct oxidation of methane in SOFCs [19].

2. Experimental

2.1. Preparation of GDC, CeO_2, $Zr_{0.1}Ce_{0.9}O_{2-\delta}$ and $Ba_{0.9}Co_{0.7}Fe_{0.2}Nb_{0.1}O_{3-\delta}$ cathode

All reagents used in this work were obtained from Beijing Chemical Reagent Company. GDC of composition $Gd_{0.1}Ce_{0.9}O_{1.95}$ was prepared following a modified gel synthesis method [27]. The stoichiometric amounts of Gd_2O_3 and $Ce(NO_3)_3 \cdot 6H_2O$ were mixed in deionised water. After it was stirred thoroughly, a cross-linking agent consisting of N,N-methylene-bisacrylamide and monomer acrylamide solution was added. The mixture was ground using a planetary ball mill for 24 h and then vacuum deaerated. After that, the ammonium persulfate and tetramethyl ethylenediamine were added as the initiating agent and catalyst, respectively. The as-prepared slurry was stirred thoroughly again and dried gradually at 120 °C. The resulting dry precursor was calcined in air at 800 °C for 2 h in order to eliminate carbonaceous residues and obtain the GDC powder. Finally, the as-prepared GDC powder was ball-milled again for 12 h to achieve average particle distribution. A similar procedure was used for the preparation of CeO_2 and $Zr_{0.1}Ce_{0.9}O_{2-\delta}$ (ZDC) powders and $Ce(NO_3)_3 \cdot 6H_2O$ and $ZrO(NO_3)_2 \cdot nH_2O$ were used as the starting reagents. $Ba_{0.9}Co_{0.7}Fe_{0.2}Nb_{0.1}O_{3-\delta}$ (BCFN) was prepared by the conventional solid state reaction process as described in our previous work [28,29]. Stoichiometric amounts of $BaCO_3$, Fe_2O_3, Co_3O_4, and Nb_2O_5 were mixed by ball-milling in ethyl alcohol medium for 48 h. Calcination of the precursor powders was performed at 1000 °C in air for 24 h. Finally, the synthesized oxide was ball-milled again for 24 h.

2.2. Fabrication of single cells

The SOFC single cells investigated in this study were typical anode-supported button cells of 0.2 cm^2 active area. They consisted of the CeO_2-based anode supports, GDC electrolytes, and BCFN cathodes. The anode substrates were fabricated using the tape casting techniques. Slurries for tape casting were prepared by ball-milling ZDC or CeO_2 powder mixing with the graphite in a weight ratio of 50:50 for 48 h with appropriate amounts of dispersant, binder, plasticizer and solvent. The resulting homogeneous slurry was then cast using a tabletop caster (DR-150, Japan). GDC electrolyte was fabricated by casting GDC slurry which was prepared in the same way as the anode substrates except that no graphite was added. The green sheets of ZDC or CeO_2 anode substrate and GDC were isostatically pressed at 16 MPa for 20 min using a thermal isostatic press (30T, Shanxi, China). The laminate was punched to discs, and then fired in air at 1500 °C for 10 h. The porosities of the sintered anode substrate were from 59% to 61% as measured by the Archimedes method. $Ni(NO_3)_2$, $Cu(NO_3)_2$ or their mixture in a molar ratio of 1:1 was infiltrated into the porous anode layer by a solution infiltration process. In order to introduce sufficient amount of metal phase into the porous substrate, multiple infiltrations were used, followed by firing at 450 °C for 1 h after each infiltration. Then the BCFN cathode was screen printed on the GDC electrolyte. Finally, the as-prepared cells were sintered at 900 °C for 5 h. The metal oxide was reduced to metal in flowing H_2 during the initial heating of the fuel cell for testing. The final metal composition for each of the anodes was about 40 wt%. For identification purpose, cells received a denomination according to the anode materials applied. Thus, cell NCZ, NZ, CZ, NCC, NC and CC represents a sample with a $Ni_{0.5}Cu_{0.5}$–ZDC, Ni–ZDC, Cu–ZDC, $Ni_{0.5}Cu_{0.5}$–CeO_2, Ni–CeO_2 and Cu–CeO_2 anode, respectively.

2.3. Physico-chemical characterization

The crystallographic phases of the CeO_2-based powders were verified by XRD analysis on a PANalytical X'Pert PRO X-ray diffractometer using Cu Kα radiation. The morphology of cells and element composition of the anodes before and after the stability test were investigated by scanning electron microscopy (SEM) using a ZEISS-EVO 18 Special Edition instrument alongside EDS (BRUKER X-FLASH DETECTOR 5010).

2.4. Electrochemical measurements

Electrical contacts were made to each of the electrodes using Ag mesh, Ag paste and Ag wire. CH_4 humidified at room temperature (~3 vol.% H_2O) was fed to the anode at a flow rate of 30 mL min^{-1}, while the cathode was exposed to ambient air. Polarization curves (I–V) of the single cells were galvanostatically measured using an Arbin test system (Arbin MSTAT4) at 700 °C. To understand the operational stability of the single cells under weakly humidified CH_4, the variation of current density with time at a constant voltage of 0.6 V was recorded for all the cells with various anode materials.

3. Results and discussion

3.1. Physico-chemical characterization of single cells

The XRD patterns of the GDC, ZDC and CeO_2 powder are presented in Fig. 1. A qualitative analysis of the XRD data suggests that all the three samples match a cubic phase (fluorite type crystal structure) and all the peaks are indexed accordingly in the figure. The absence of other peaks indicates that any additional phases are present below the detection limit of the XRD experiment and that the CeO_2-based materials are therefore of high phase-purity.

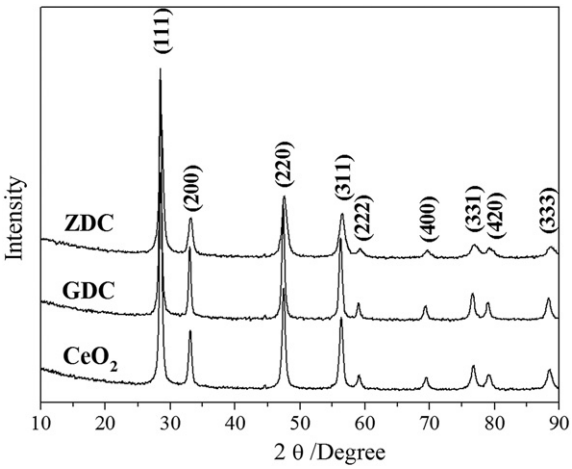

Fig. 1. XRD patterns of GDC, ZDC and CeO_2 powder.

Typical SEM images of the $Ni_{0.5}Cu_{0.5}$–ZDC anode surface and cross-section of electrode–electrolyte interfaces in the NCZ cell are shown in Fig. 2. In Fig. 2a, the nano-particles of Ni–Cu oxides are

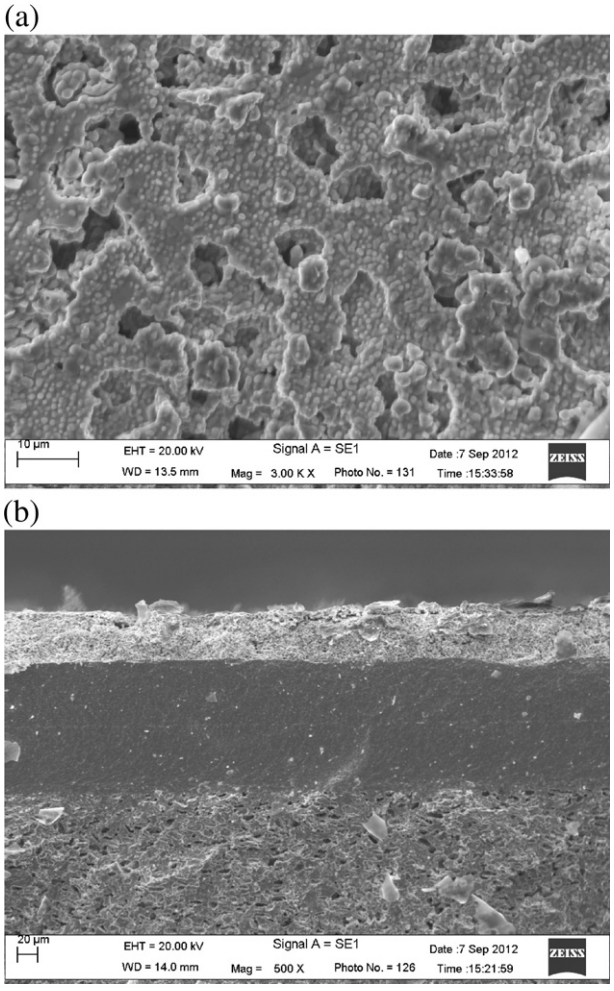

Fig. 2. Typical SEM images of (a) the $Ni_{0.5}Cu_{0.5}$–ZDC anode surface and (b) the electrode–electrolyte region in cross-section of a $Ni_{0.5}Cu_{0.5}$–ZDC anode-supported SOFC cell.

uniformly and sufficiently coated in the porous ZDC backbone. The GDC electrolyte appears to be dense and has a mean thickness of 80 μm, as shown in Fig. 2b. Both the electrode layers exhibit a highly porous microstructure and the interfaces between the electrodes and electrolyte show no separation, indicating good contact and adhesion between these layers. The thickness of cathode is approximately 40 μm. Estimated porosity for the anode and cathode is about 40% and 30%, respectively. The geometrical area of the cathode is 0.2 cm^2.

3.2. Electrochemical characterization

3.2.1. Single cell performances

Fig. 3 shows the performances of the single cells using various anodes at 700 °C under humidified CH_4. The open circuit voltages (OCVs) of the cells using Ni-containing anodes are obviously higher than those using Cu–cermet anodes, as shown in Table 1. The OCV of cell using MIEC as the solid electrolyte can be expressed as [30]

$$V_{OC} = V_{th} - I_i R_i - \eta_a - \eta_c \quad (1)$$

where V_{OC} is the measured open circuit voltage, V_{th} is the theoretic voltage, I_i is the internal ionic current, R_i is the inoic resistance of the electrolyte, η_a is the anodic overpotential and η_c is the cathodic overpotential.

V_{OC} can also be expressed as [31]

$$V_{OC} = \frac{R_e}{R_e + R_{p(a)} + R_i + R_{p(c)}} V_{th} \quad (2)$$

where R_e is the electronic resistance of electrolyte, $R_{p(a)}$ and $R_{p(c)}$ are the polarization resistances of anode and cathode.

Eqs. (1) and (2) show that the properties of electrodes also determine the V_{OC} besides that of MIEC electrolyte. Since the electrolyte and cathode materials for all the cells are seemingly the same, we speculate that the difference in V_{OC} is mainly caused by the difference in polarization at anode/electrolyte interface, which can reflect the difference in the activities of anodes. McIntosh and Gorte [32] have pointed out that the slow surface kinetics could also result in the surface at the anode/electrolyte interface not being in equilibrium and the partial oxidation products that remain on the anode surface or nonelectrochemical surface reactions can lower the OCV of SOFCs using methane. Thus, it is deduced that the cells using Cu–cermet anodes may have lower activities for surface reactions than Ni-containing anodes. The trend of polarization and power density curves confirms that both the cells using Cu–ZDC and Cu–CeO_2 anodes show low performances. The cells with Ni-containing anodes exhibit nearly three times higher performance than those with Cu–cermet anodes. Ni possesses a high catalytic activity for direct oxidation and for steam reforming of methane. However, Cu is not a good catalyst for those reactions. McIntosh et al. [31,33] have reported that the performance of CeO_2-based anodes can be largely increased by adding Pd which is highly active for CH_4 cracking.

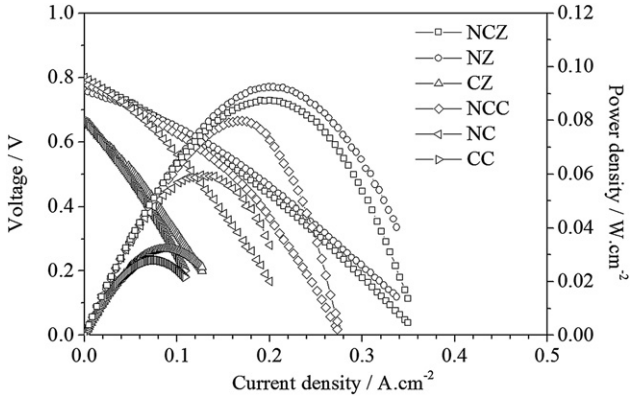

Fig. 3. Polarization and power density curves at 700 °C under 97%CH_4/3%H_2O and stationary air for the cells using different anodes.

Table 1
Performances of SOFC single cells.

Cell	NCZ	NZ	CZ	NCC	NC	CC
OCV (V)	0.793	0.759	0.660	0.785	0.799	0.670
MPD (W cm^{-2})	0.087	0.092	0.032	0.080	0.060	0.028

All the cells with ZDC based anodes give a significant increase in power density in comparison with those using pure CeO_2-based anodes at 700 °C under 97%CH_4/3%H_2O. This result is in a good agreement with the impedance studies of ZDC anodes, which depict that by doping 10 mol% Zr into CeO_2, the anode activity for electrochemical oxidation of CH_4 can be improved [19]. Ce-based oxides can store oxygen when they are in contact with an oxidant atmosphere, and release oxygen when they are in the presence of a reducing atmosphere. This process is sustained by the Ce^{4+}/Ce^{3+} redox couple. Adding Zr^{4+} into the cubic fluorite phase CeO_2, Ce^{4+} can be reduced more easily and thereby effectively increase the concentration of Ce^{3+} and OSC [16]. Laosiripojana et al. [34] investigated the steam reforming of methane over Ni on high surface area CeO_2 and ZDC supports. They observed that Ni/ZDC showed better performance and resistance toward carbon formation than Ni/CeO_2 catalyst, which was attributed to the higher OSC of ZDC than CeO_2. The cubic phase ZDC oxide is a well-known oxygen storage material [35,36]. However, the tetragonal phases of ZDC oxides are not active in oxygen storage [37]. Baker et al. have systematically investigated the preparation [38], crystallite structure [38], catalytic activity [39] and electrochemical anodic activity of ZDC materials [19]. They found that ZDC solid solutions with CeO_2 content up to 75 mol% exhibited a tetragonal structure ($P42/nmc$ space group), whereas the $Zr_{0.1}Ce_{0.9}O_{2-\delta}$ exhibited a cubic structure ($Fm3m$ space group). Larrondo et al. [16] also reported that the ZDC oxide with 10% mol Zr exhibited a cubic phase but those with 30% mol and 50% mol Zr presented tetragonal phases. Huber [40] and Terribile [41] reported that the catalytic activity of pure ceria for total oxidation of methane could be enhanced by substituting ZrO_2 into ceria. The best redox properties and highest OSC for ZDC was obtained at relatively low Zr content. As the XRD pattern of the $Zr_{0.1}Ce_{0.9}O_{2-\delta}$ powder presents a cubic phase in Fig. 1, the promotion in OSC and oxygen mobility by adding 10% mol Zr into CeO_2 is considered as one of the reasons for the improvement in anode activity.

Furthermore, He et al. [9] found that the anode performance also depended strongly on CeO_2 particle size and morphology for Cu–CeO_2-based anode. The maximum power densities of the SOFCs decreased with calcination temperature of the anode materials. They concluded the decreased performance was more likely associated with catalytic properties. The studies on the thermal stability of CeO_2 have demonstrated that it can deactivate from sintering at high temperature, particularly under a reducing atmosphere [42]. To avoid this problem, the addition of ZrO_2 to CeO_2 can effectively impede the growth of ceria particles, resulting in a higher stability than pure CeO_2 [43]. In contrast to the significant impact of calcination temperature on the catalytic activity for CeO_2, ZDC shows relatively refractory. The specific area value of $Zr_{0.1}Ce_{0.9}O_{2-\delta}$ calcinated at 800 °C was same as that calcinated at 600 °C, and the former could present a better performance for oxidation of methane. The good thermal stability of ZDC

at high temperature under reducing conditions is thought to be another reason for the increase in anode performance.

The NZ cell shows the highest performance within all the cells investigated, about 0.092 W cm^{-2} at 700 °C under weakly humidified CH_4. The performance difference between the NZ cell and NCZ cell is slight, indicating a comparable activity for the $Ni_{0.5}Cu_{0.5}$–ZDC anode and Ni–ZDC anode. However, the performance of NC cell is obviously lower than that of the NCC cell. The performance difference between these two cells is greater than that between the NCZ and NZ cells, which was likely due to the severe carbon deposition on the Ni–CeO_2 anode during the performance test. However, the carbon deposition might have been effectively mitigated on the $Ni_{0.5}Cu_{0.5}$–CeO_2 anode. The studies on Ni–Cu alloys based anodes for direct hydrocarbon SOFCs have demonstrated that carbon deposition can be substantially suppressed by addition of Cu and the stable operation of cells can be maintained for a long time [21–23,44]. This will be further discussed in the following stability examination. Considering the thickness of GDC electrolyte is as high as 80 μm, the cell performances should be enhanced by employing a thinner GDC membrane which can reduce the cell resistance. Further work on the optimization of anode composition and cell structure is being conducted and will be reported elsewhere.

3.2.2. Stability of single cells

Adequate thermal stability of anodes under reducing conditions, besides the high electrochemical activity for oxidation of hydrocarbon, is another essential requirement for direct hydrocarbon SOFCs. The anode should suppress the carbon deposition and maintain a stable activity during the operation. Short-term stability tests for all the cells at 700 °C were conducted at a constant voltage of 0.6 V under 97%CH_4/3%H_2O. Fig. 4 shows the variation of current density with time for various cells. Both the NZ cell and NC cell show rapid degradation during the test, as shown in Fig. 4a and b. The current density for the NZ cell decreases 55% after 10 h and that for the NC cell degrades 74% after only 40 min test, which indicates that the thermal stability for Ni–ZDC anode is relatively higher than Ni–CeO_2 anode. Fig. 4c and d shows that the NCZ cell degrades only 3.8% after 48 h, whereas the NCC cell degrades 10.5% after 24 h test, which further demonstrates that by doping 10 mol% Zr into CeO_2, the thermal stability of anode can be improved. Additionally, both the NCC and NCZ cells exhibit better stabilities than NC and NZ cells, suggesting a higher stability of Ni–Cu alloy with respect to Ni for oxidation of methane. Cu–cermet anodes exhibit the highest stabilities. The CC cell degrades only 2.4% after 48 h, and the CZ cell shows the lowest degradation, only 0.61% after 48 h test, as shown in Fig. 4e and f.

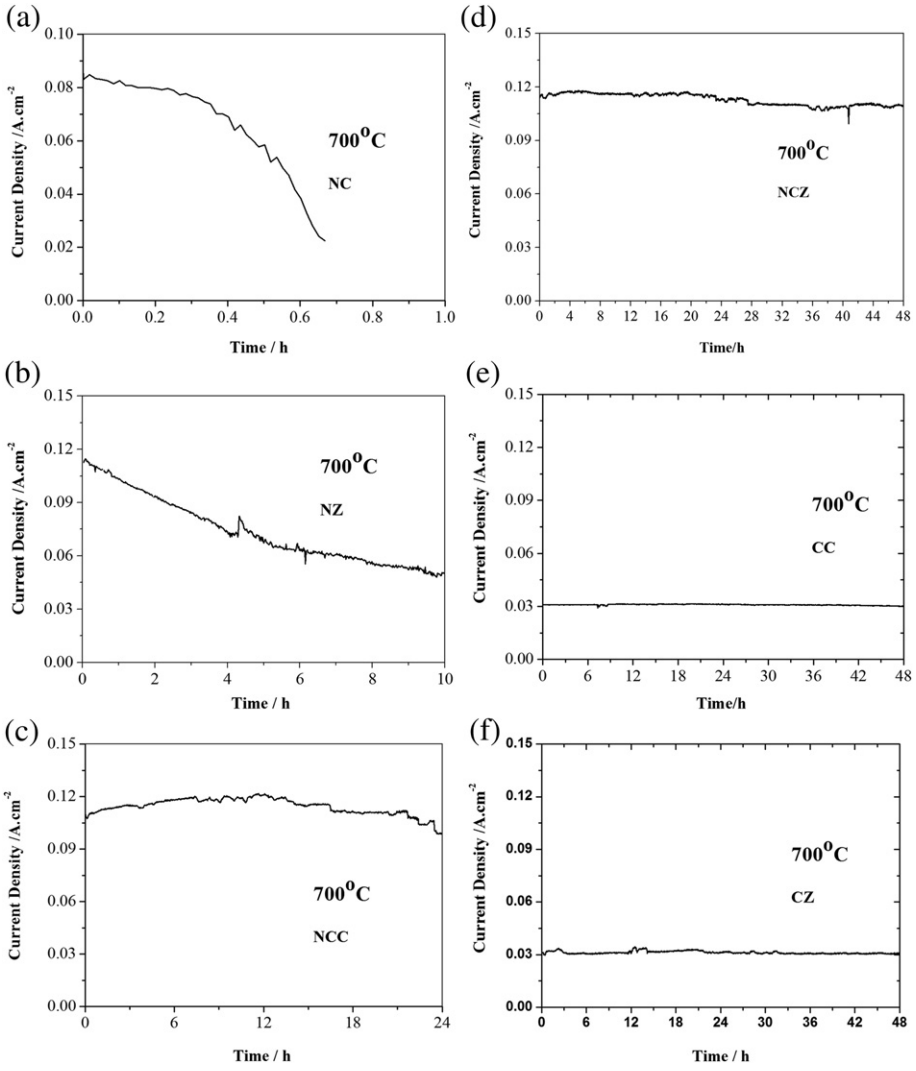

Fig. 4. The variation of current density with time at 0.6 V for (a) the NC cell, (b) the NZ cell, (c) the NCC cell, (d) the NCZ cell, (e) the CC cell and (f) the CZ cell at 700 °C under 97% CH_4/3%H_2O.

SEM/EDS analyses are conducted for all the anodes after the stability tests. Fig. 5 shows the morphologies of anode surfaces after test. The line frames in the images show the areas of the EDS analysis. The carbon contents calculated from the EDS analysis are listed in Table 2. Carbon deposition can be clearly observed on Ni cermet anodes, resulting in a significant decrease in porosity, as shown in Fig. 5a and b. Fig. 5c and d shows that Ni–Cu alloy based anodes are more porous than Ni cermet anodes after test. However, carbon deposition can still be found in comparison with the microstructure of anode before test, as shown in Fig. 2a. The microstructure of Cu–cermet anodes is found to maintain very well in Fig. 5e and f. The carbon contents shown in Table 2 verify that the Cu–cermet anodes possess the highest resistance to carbon deposition. For all the ZDC based anodes, carbon deposition can be obviously suppressed, which indicates that ZDC could be a promising anode material for direct hydrocarbon SOFCs. The $Ni_{0.5}Cu_{0.5}$–ZDC anode can achieve a comparable stability to the Cu–cermet anodes and a high activity as good as Ni cermet anodes.

Direct oxidation of hydrocarbons in an SOFC requires all the steps in anode process to be involved in electrochemical reaction. Accordingly, the anode process including cracking of the hydrocarbon and the subsequent electrochemical oxidation of the cracking products cannot be defined as direct oxidation, though it has been considered to occur generally in a direct hydrocarbon SOFC [32]. The definition of direct utilization, rather than direct oxidation of hydrocarbons, which the hydrocarbons are fed to the SOFCs directly without significant amounts of water or other oxidants, such as CO_2 and oxygen may be more applicable [32]. Dry or weakly humidified hydrocarbons at room temperature (~3 vol.% H_2O) are generally employed for direct hydrocarbon SOFCs. Due to the very low water content, the steam reforming activity would be very low. Thus, for a direct methane SOFC, the deposited carbon either via reactions over a catalyst or by pyrolysis of CH_4 would lead to a rapid degradation of anode activity. For an SOFC operated at IT, the former mechanism of carbon deposition related to surface reactions may play a more important role in anode deactivation process. Wang et al. [45] reported that GDC-impregnated Ni anode was very stable under weakly humidified (~3 vol.% H_2O) methane at 800 °C, due to the re-oxidation of carbon deposited on the Ni surface by the nano-sized GDC particles. He and Hill [46] placed $Zr_{0.25}Ce_{0.75}O_2$ pellets on each side of the Ni/YSZ pellet and investigated the carbon deposition under methane humidified at room temperature for 4 h. The amount of carbon deposition can be significantly reduced by addition of a ZDC layer and the Ni/YSZ structure was not irreversibly changed. Sumi et al. [47] evaluated the performance of a 300-μm-thick ScSZ electrolyte supported SOFC with a Ni–ScSZ anode using 97%CH_4/3%H_2O and oxygen as the fuel and oxidant, respectively. The cell showed 0.85 W cm^{-2} of the power density at 0.85 V at 1000 °C and no degradation during 250 h operation at a constant current of 1.0 A cm^{-2}. Huang et al. [48] examined the performance of an SOFC with a GDC coated Ni/ScSZ anode support and a 15-μm-thick ScSZ electrolyte under 97% CH_4/3%H_2O. The maximum power density (MPD) was 224 mW cm^{-2} at 700 °C and the electrochemical impedance spectra showed no significant degradation in electrode polarization resistance during 84 h stability test under open circuit. The additional ceria/zirconia interfaces was regarded to increase the methane oxidation rates by enhancing oxygen storage. Lv et al. [49] operated an LSGM electrolyte supported cell with a $Ce_{0.8}Fe_{0.2}O_{2-\delta}$ anode under 97%CH_4/3%H_2O. The MPD was 33 mW cm^{-2} at 700 °C. The electrode polarization resistance only increased mildly with time and little carbon deposition was found during the stability test at 800 °C for 20 h. Murry et al. [2] fabricated an LSM cathode supported SOFC with an 8-μm-thick YSZ electrolyte and a CeO_2-based anode using magnetron sputtering. The cell could achieve a similar performance for using dry and wet (with 3% H_2O) methane. Cell performance was stable under dry methane for 100 h life test, whereas a stable operation under wet methane at low voltages was not successful due to Ni anode being oxidized. Gorte et al. [50] investigated an SOFC with a Cu–CeO_2-based anode and a 60-μm-thick YSZ electrolyte. The MPD of the cell using dry methane at 700 °C was 0.09 W cm^{-2}. The cell could achieve a stable

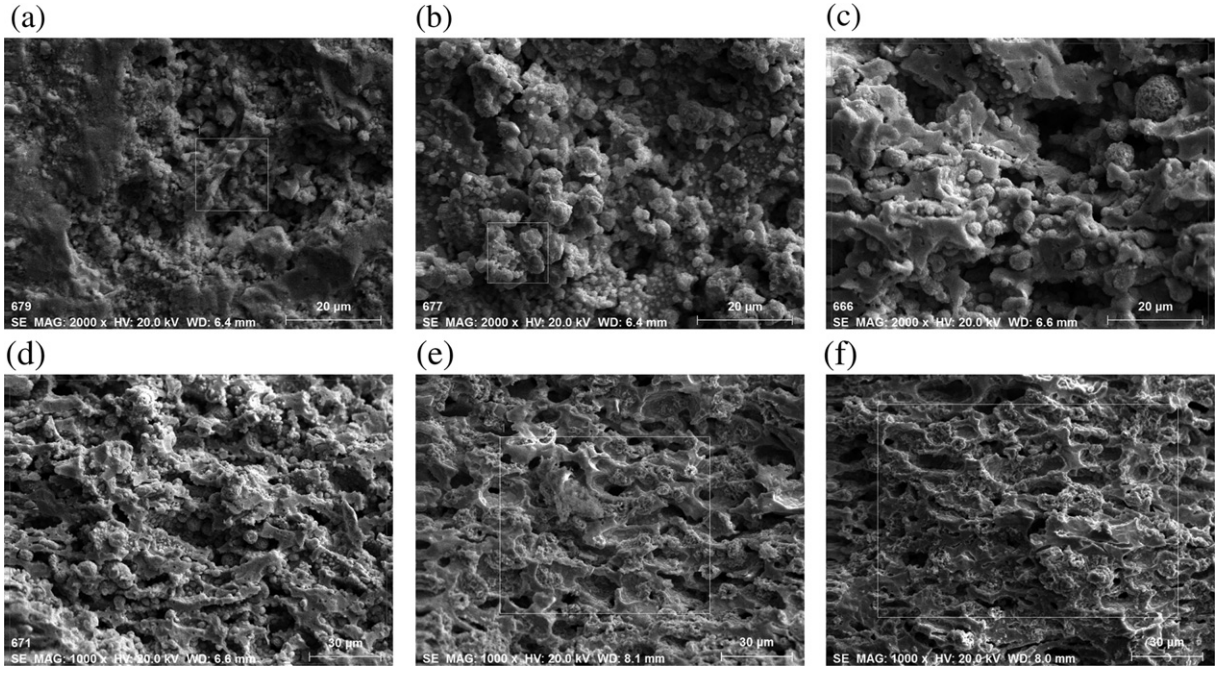

Fig. 5. Typical SEM images of the surface of (a) Ni–CeO_2 anode, (b) Ni–ZDCanode, (c) $Ni_{0.5}Cu_{0.5}$–CeO_2 anode, (d) $Ni_{0.5}Cu_{0.5}$–ZDC anode, (e) Cu–CeO_2 anode, (f) Cu–ZDC anode after the stability test under 97%CH_4/3%H_2O, the line frames in the images show the areas of the EDS analysis.

Table 2
Carbon content on anode surfaces after stability test.

Anode	Ni–CeO_2	Ni–ZDC	$Ni_{0.5}Cu_{0.5}$–CeO_2	$Ni_{0.5}Cu_{0.5}$–ZDC	Cu–CeO_2	Cu–ZDC
C content (wt%)	15.62	10.72	4.93	2.88	2.19	1.93

performance for at least three days when operated at maximum power under n-butane at 700 °C. However, when it was operated at open circuit for a 2 h period, the OCV decreased from 0.95 V to 0.87 V.

It may be difficult to compare the anode performances and stabilities for direct methane SOFCs in the literature because of the different materials and microstructures of the electrodes and electrolyte used, and the various reducing conditions and fuel utilizations applied. Nevertheless, it is clear that NiCu-ZDC based anodes do show very impressive performances and stabilities for direct utilization of methane in IT-SOFCs.

4. Conclusions

In studies on direct methane SOFCs using $Zr_{0.1}Ce_{0.9}O_{2-\delta}$ based anode materials, significant improvements in performances and thermal stabilities were observed in comparison with that using pure CeO_2-based anodes at 700 °C. This result indicates that by doping 10 mol% Zr into CeO_2, both the thermal stability and activity of anode could be improved. The best performing cell was that with Ni–$Zr_{0.1}Ce_{0.9}O_{2-\delta}$ anode. A short-term stability test verified that Cu–cermet anodes possessed better resistance to carbon deposition than Ni-containing anodes. Cu–$Zr_{0.1}Ce_{0.9}O_{2-\delta}$ anode presented the lowest degradation in performance, only 0.61% after 48 h operation in 97%CH_4/3%H_2O, but a low performance as well. The $Ni_{0.5}Cu_{0.5}$-$Zr_{0.1}Ce_{0.9}O_{2-\delta}$ anode could achieve a comparable stability to Cu–$Zr_{0.1}Ce_{0.9}O_{2-\delta}$ anode and a high activity as good as Ni–$Zr_{0.1}Ce_{0.9}O_{2-\delta}$ anode. It is concluded that the NiCu–$Zr_{0.1}Ce_{0.9}O_{2-\delta}$ based cermets could be promising candidate anodes for direct hydrocarbon IT-SOFCs.

Acknowledgements

This project was sponsored by financial supports from Program for New Century Excellent Talents in Universities in China, National Basic Research Program of China (973 Program), No. 2012CB215400 (2012CB215406) and Scientific Research Foundation for the Returned Overseas Chinese Scholars.

References

[1] B.C.H. Steele, Nature 400 (1999) 619–621.
[2] E.P. Murray, T. Tsai, S.A. Barnett, Nature 400 (1999) 649–651.
[3] S. Park, J.M. Vohs, R.J. Gorte, Nature 404 (2000) 265–267.
[4] S. Park, R. Craciun, J.M. Vohs, Raymond J. Gorte, J. Electrochem. Soc. 146 (10) (1999) 3603–3605.
[5] S. McIntosh, J.M. Vohs, R.J. Gorte, J. Electrochem. Soc. 150 (10) (2003) A1305–A1312.
[6] S. Tao, John T.S. Irvine, Nat. Mater. 2 (2003) 320–323.
[7] J.C. Ruiz-Morales, J. Canales-Vazquez, C. Savaniu, D. Marrero-Lopez, W. Zhou, J.T.S. Irvine, Nature 439 (2006) 568–571.
[8] Y.-H. Huang, R.I. Dass, Z.-L. Xing, J.B. Goodenough, Science 312 (2006) 254–257.
[9] H. He, J.M. Vohs, R.J. Gorte, J. Electrochem. Soc. 150 (1) (2003) A1470–A1475.
[10] R. Di Monte, J. Kaspar, J. Mater. Chem. 15 (2005) 633–648.
[11] A. Martínez-Arias, A.B. Hungría, M. Fernández-García, A. Iglesias-Juez, J.C. Conesa, G.C. Mather, G. Munuera, J. Power Sources 151 (2005) 43–51.
[12] F.J. Pérez-Alonso, M. López Granados, M. Ojeda, P. Terreros, S. Rojas, T. Herranz, J.L.G. Fierro, Chem. Mater. 17 (2005) 2329–2339.
[13] G. Li, R.I. Smith, H. Inomata, J. Am. Chem. Soc. 123 (2001) 11091–11092.
[14] A.C. Tavares, B.L. Kuzin, S.M. Beresnev, N.M. Bogdanovich, E.Kh. Kurumchin, Y.A. Dubitsky, A. Zaopo, J. Power Sources 183 (2008) 20–25.
[15] M. Boaro, A. Trovarelli, Jin-Ha Hwang, T.O. Mason, Solid State Ionics 147 (2002) 85–95.
[16] S. Larrondo, M.A. Vidal, B. Irigoyen, A.F. Craievich, D.G. Lamas, I.O. Fábregas, G.E. Lascalea, N.E.W. de Reca, N. Amadeo, Catal. Today 107-108 (2005) 53–59.
[17] K. Ahn, H. He, J.M. Vohs, R.J. Gorte, Electrochem. Solid-state Lett. 8 (8) (2005) A414–A417.
[18] M. Cimenti, V. Alzate-Restrepo, J.M. Hill, J. Power Sources 195 (2010) 4002–4012.
[19] S. Song, R.O. Fuentes, R.T. Baker, J. Mater. Chem. 20 (2010) 9760–9769.
[20] M. Daturi, E. Finocchio, C. Binet, J.-C. Lavalley, F. Fally, V. Perrichon, H. Vidal, N. Hickey, J. Kašpar, J. Phys. Chem. B 104 (2000) 9186–9194.
[21] G. Bonura, C. Cannilla, F. Frusteri, Appl. Catal. B: Environ. 121–122 (2012) 135–147.
[22] W. An, D. Gatewood, B. Dunlap, C.H. Turner, J. Power Sources 196 (2011) 4724–4728.
[23] A. Sin, E. Kopnin, Y. Dubitsky, A. Zaopo, A.S. Aricò, D. La Rosa, L.R. Gullo, V. Antonucci, J. Power Sources 164 (2007) 300–305.
[24] R.J. Gorte, J.M. Vohs, J. Catal. 216 (1–2) (2003) 477–486.
[25] Y.M. Choi, C. Compson, M.C. Lin, M. Liu, J. Alloys Compd. 427 (2007) 25–29.
[26] G. Chen, G. Guan, S. Abliz, Y. Kasaid, A. Abudula, Electrochim. Acta 56 (2011) 9868–9874.
[27] M. Han, W. Li, Chinese patent, no. CN101575214.
[28] S. Song, P. Zhang, M. Han, S.C. Singhal, J. Membr. Sci. 415–416 (2012) 654–662.
[29] Z. Yang, C. Yang, B. Xiong, M. Han, F. Chen, J. Power Sources 196 (2011) 9164–9168.
[30] I. Riess, J. Electrochem. Soc. 128 (1981) 2077–2081.
[31] W. Lai, S.M. Haile, Phys. Chem. Chem. Phys. 10 (2008) 865–883.
[32] S. McIntosh, R.J. Gorte, Chem. Rev. 104 (2004) 4845–4865.
[33] S. McIntosh, J.M. Vohs, R.J. Gorte, Electrochem. Solid-state Lett. 6 (2003) A240–A243.
[34] N. Laosiripojana, D. Chadwick, S. Assabumrungrat, Chem. Eng. J. 138 (2008) 264–273.
[35] J.R. Gonzalez-Velasco, M.A. Gutierrez-Ortiz, J.L. Marc, J.A. Botas, M.P. Gonzalez-Marcos, G. Blanchard, Appl. Catal. B: Environ. 22 (1999) 167–178.
[36] J. Beckers, F. Clerc, J.H. Blank, G. Rothenberg, Adv. Synth. Catal. 350 (2008) 2237–2249.
[37] F. Zhang, C.-H. Chen, J.M. Raitano, J.C. Hanson, W.A. Caliebe, S. Khalid, S.-W. Chan, J. Appl. Phys. 99 (2006) 084313-1–084313-8.
[38] R.O. Fuentes, R.T. Baker, J. Phys. Chem. C. 113 (2009) 914–924.
[39] J. Kearney, J.C. Hernandez-Reta, R.T. Baker, Catal. Today 180 (1) (2012) 139–147.
[40] F. Huber, H. Venvik, M. Ronning, J.C. Walmsley, Chem. Eng. J. 137 (3) (2008) 686–702.
[41] D. Terribile, A. Trovarelli, C. de Leitenburg, A. Primavera, G. Dolcetti, Catal. Today 47 (1) (1999) 133–140.
[42] V. Perrichon, A. Laachir, S. Abouarnadasse, O. Touret, G. Blanchard, Appl. Catal. A 129 (1995) 69–82.
[43] A. Trovarelli, C. de Leitenburg, G. Dolcetti, Chem. Tech. 27 (1997) 32–37.
[44] Z. Xie, C.R. Xia, M.Y. Zhang, W. Zhu, H.T. Wang, J. Power Sources 161 (2006) 1056–1061.
[45] W. Wang, S.P. Jiang, A.I.Y. Tok, L. Luo, J. Power Sources 159 (2006) 68–72.
[46] H. He, J.M. Hill, Appl. Catal. A: Gen. 317 (2007) 284–292.
[47] H. Sumi, K. Ukai, Y. Mizutani, H. Mori, C.-J. Wen, H. Takahashi, O. Yamamoto, Solid State Ionics 174 (2004) 151–156.
[48] B. Huang, X.F. Ye, S.R. Wang, H.W. Nie, J. Shi, Q. Hu, J.Q. Qian, X.F. Sun, T.L. Wen, J. Power Sources 162 (2006) 1172–1181.
[49] H. Lv, D.J. Yang, X.M. Pan, J.S. Zheng, C.M. Zhang, W. Zhou, J.X. Ma, K.A. Hu, Mater. Res. Bull. 44 (2009) 1244–1248.
[50] R.J. Gorte, S. Park, J.M. Vohs, C. Wang, Adv. Mater. 12 (19) (2000) 1465–1469.